FLOW PATTERNS AND DRAG COEFFICIENTS
OF CEPHALOPOD SHELLS

by JOHN A. CHAMBERLAIN

ABSTRACT. Streamlining is important in the adaptive strategy of swimmers because it minimizes waste of propulsive energy (i.e. maximizes hydrodynamic efficiency). Streamlining of cephalopod shell form was evaluated by analysing the pattern of fluid flow past shells and by calculating shell drag coefficients. Flow visualization experiments show that shell flow patterns are characterized by boundary layer separation along the flank of the outer whorl, and by turbulence in the umbilicus and behind the shell. Tow-tank measurement of drag and velocity shows that variation in shell geometry causes significant variation in drag coefficient. Inflated, depressed, and widely umbilicate shells have high drag coefficients (generally greater than 0·6–0·7). Shells that delay separation (e.g. compressed, involute oxycones) have low drag coefficients (about 0·1), but this is more than an order of magnitude greater than drag coefficients of rapid-swimming fish and squids. For most shell types change in shell orientation during swimming results in slightly higher drag coefficients as velocity increases. Analogy with aircraft and ship appendages suggests that extension of the body behind the shell has virtually no effect on drag coefficient.

FOR most animals mode of life and locomotion are so closely interwoven that the two terms are practically synonymous. Not surprisingly, locomotion has become a key issue in interpreting the mode of life of fossil ectocochliate cephalopods (ammonoids and nautiloids). Interest in the locomotion of fossil cephalopods has focused on swimming. How well did ectocochliates swim? How can the fossil record be used to evaluate swimming ability in this remarkable group of animals?

Although much has been learned about cephalopod swimming from studies relying on such palaeontological evidence as: trace fossils (Flower 1955); epizoans (Seilacher 1960, 1968; Merkt 1966; Meischner 1968; Petriconi 1971); colour patterns (Ruedemann 1921; Foerste 1930; Spath 1935); shell abnormalities (Roll 1935; Bayer 1970); shell strength (Westermann 1973); anatomical structures (Mutvei 1964; Lehmann 1971; Mutvei and Reyment 1973); and biofacies relationships (Scott 1940; Westermann 1954), information on swimming ability provided by these works is generalized or qualitative. Since swimming is a hydrodynamic process, one way to deal directly and quantitatively with the problem of cephalopod swimming ability is to analyse the hydromechanical properties of the shell. One obvious property is shell streamlining because streamlining and swimming ability are directly related to one another (Hertel 1966; Alexander 1967, 1968), and because the shell is the only ectocochliate body part commonly preserved in the fossil record.

Previous studies on shell streamlining (Schmidt 1930 and Kummel and Lloyd 1955) illustrate the practicality and informativeness of this approach. Kummel and Lloyd used a circulating water channel and balance system to determine the 'relative drag coefficients' of plaster casts of twenty species of coiled ectocochliates. Their data suggest that streamlining varies with shell form, and thus that fossil cephalopods may have displayed considerable difference in swimming ability. However, further research is needed to clarify relationships between shell form, streamlining,

and swimming ability, and to develop a more thorough understanding of the role of streamlining in the adaptive strategy of fossil cephalopods.

This paper presents the results of experiments on patterns of flow around cephalopod shells and also measurement of drag coefficient for a wide range of shell types. The objectives were first to see how drag is produced by a shell, and secondly to determine how shell geometry, shell orientation, and body extension influence drag coefficient. Subsequent work will consider the effect of shell sculpture on drag coefficient, and examine swimming ability and the adaptive significance of shell form.

SWIMMING, STREAMLINING, AND DRAG COEFFICIENT

The velocity of any self-propelled body with a limited source of propulsive energy is a function of its hydrodynamic efficiency, i.e. the efficiency with which its thrust is converted to velocity. For aquatic animals of the size of cephalopods, hydrodynamic efficiency is determined by body morphology. Body forms that generate little drag conserve a swimmer's energy expenditures, while forms which cause much drag waste energy. The relation between these variables is given by:

$$D_F = \tfrac{1}{2}\rho V^2 A C_D \qquad \text{(Eq. 1)}$$

where D_F is drag force; ρ is fluid density; V is swimming velocity; A is an area representative of the animal; and C_D is the drag coefficient. A can be thought of as representing body size, and C_D as representing body shape. Since thrust equals drag when velocity is constant, C_D is an index of a body's hydrodynamic efficiency.

The magnitude of the drag coefficient is a function of the degree to which body form inhibits undisturbed flow around a swimming animal. Well streamlined animals produce minimal drag because their slender, fusiform bodies cause little flow disruption. They have small drag coefficients, and are highly efficient. Conversely, poorly streamlined animals cause much disruption, and have larger drag coefficients and low efficiencies. Streamlining and flow disruption for inanimate bodies of various shapes are diagrammed in text-fig. 1.

Streamlining and hydrodynamic efficiency are factors of considerable importance to aquatic animals. Virtually all rapid swimmers, regardless of their mode of propulsion or phylogenetic relationships, have well-streamlined, highly efficient body shapes (Hertel 1966). Conservation of locomotive energy is not so critical a need among poor swimmers, and hence such animals are invariably poorly streamlined and less efficient. The ubiquitous need for rapid swimming organisms to utilize their limited locomotive energy supply in the most economical way ensures that this correlation between body morphology and swimming ability extends to ectocochliates. We should thus be able to obtain a good idea of cephalopod swimming ability by measuring shell drag coefficients.

EXPERIMENTAL METHODS

The experimental portion of this work consists of determining drag coefficients and mapping flow patterns using instruments and procedures commonly employed in
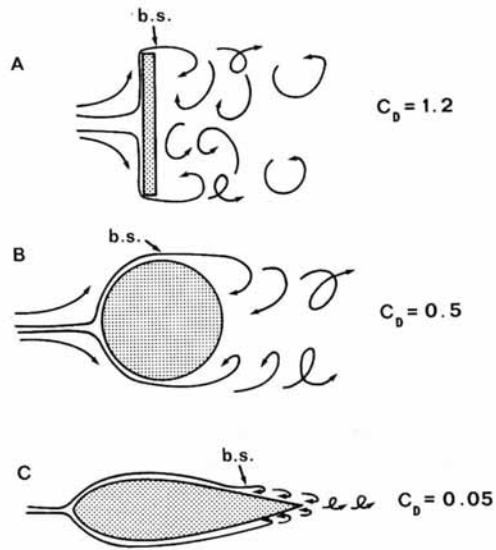
TEXT-FIG. 1. Flow fields around three bodies of different shape in subcritical flow, i.e. Reynolds number $< 5 \times 10^5$ (Reynolds number $=$ (body length . velocity)/kinematic viscosity). A, flat plate held perpendicular to flow; B, sphere; C, wing.

studies on applied fluid dynamics. These are: 1, measurement of drag force and velocity; and 2, flow visualization. Shell scale models were used in the experiments instead of actual shells because the models are morphologically less complex, and as a result more easily analysed.

Scale models of cephalopod shells. Thirty-four plexiglas shell models were constructed following the technique previously described (Chamberlain 1969). Morphological differences between the models are restricted to variation in two shell parameters. Other shell characteristics, although commonly variable among real shells, are held constant in the models. The form of each model adheres to the logarithmic paradigm; ontogenetic variation in shell shape does not occur. The morphological variables are:

1. Whorl expansion rate (W)—roughly equivalent to whorl inflation;
2. Distance of the whorls to the coiling axis (D)—roughly equivalent to the size of the umbilicus.

W and D are two of the four parameters used by Raup (Raup 1961, 1962, 1966; Raup and Michelson 1965) in describing basic geometry of coiled shells, and are

defined in text-fig. 2. All models have a unique combination of W and D, but are identical to one another in other respects. The morphological constants are:

1. Relative whorl thickness (S)—models have circular whorl sections ($S = 1$); whorl height = whorl width;
2. Translation rate (T)—all models are planispiral ($T = 0$);
3. Flank position (F)—all models have their greatest whorl width at the mid-point of whorl height;
4. Surface relief—all models are smooth surfaced, none have ribs, spines, or aperture adornments;
5. Size—all models have maximum diameters of 12·7 cm.
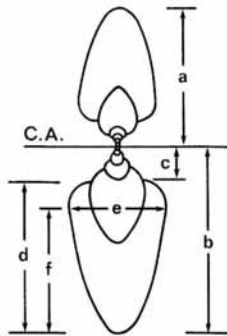
TEXT-FIG. 2. Definition of geometric parameters of shell form. $W = (b/a)^2$; $D = (b-d/b)$; $S = (e/d)$; $F = f/(b+a)$.

S, T, and F are defined in text-fig. 2. S and T are the other two geometric parameters of Raup, and along with W and D are discussed more fully in his previously cited papers. It should be stressed that since the form of each model is defined parametrically all models have strictly hypothetical morphologies. None are patterned after real prototypes, although many closely approximate shells of actual species. Table 1 gives values of W, D, S, and F for each specimen used in this experiment.

Two models (35 and 36 in Table 1) have compressed whorl sections ($S < 1$), and hence closely resemble the discoid form of oxycones. Otherwise they are identical to the thirty-four models used in the main experiment. In addition, drag and velocity measurements were made for the shell of an adult *Nautilus pompilius*. Although this treatment of variation in whorl shape obviously deals with only a token sample of the total range in this variable, it should indicate the magnitude of streamlining differences to be expected between compressed and depressed shells. Results of a more detailed analysis of the effect of whorl shape on drag coefficient will be presented in due course.

Drag and velocity measurement. It is clear from equation 1, that drag coefficient may be calculated from known values of D_F, V, ρ, and A. The density of water is known, and the representative area can be determined from the equations of Raup and Chamberlain (1967) for shell volume (shell volume raised to the 2–3 power is used as a representative area), or by water displacement. Only drag force and velocity need be determined experimentally.

To measure these two parameters, the tow tank at the Ship Hydromechanics Laboratory of the United States Naval Academy was used. A remote-controlled carriage is fitted to an overhead monorail and lateral drive rail, and moves along the length of the tank at velocities up to about 10 m/sec. Objects to be tested are suspended from the carriage, and dragged through the water. Drag force is measured by an electronic device which records distortion in the carriage frame resulting from drag on the towed object. A photocell system mounted at one end of the tank measures carriage velocity which is pre-set. Drag and velocity are continuously monitored throughout the run, and the data digitized and recorded electronically. Thirty to

TABLE 1. Geometric parameters and drag coefficients of specimens studied. All are models, except 37 which is a *Nautilus* shell.

| Specimen (model number)	Shell geometry				C_D in 30° Att.	Calc. rest Att.	C_D in rest Att.	Other Att.	C_D in other Att.
	W	D	S	F					
1	1·5	0·1	1·0	0·25	0·39	120	0·37		
2	2·0	0·1	1·0	0·26	0·52	63	0·48		
3	2·5	0·1	1·0	0·28	0·57	38	0·48		
4	3·0	0·1	1·0	0·29	0·66	24	0·58		
5	3·5	0·1	1·0	0·29	0·63	16	0·75		
6	4·0	0·1	1·0	0·30	0·64	10	0·77		
7	4·5	0·1	1·0	0·31	0·67	5	0·85		
8	5·0	0·1	1·0	0·31	0·69	1	0·95		
9	1·5	0·2	1·0	0·22	0·54	122	0·51		
10	2·0	0·2	1·0	0·23	0·57	65	0·49		
11	2·5	0·2	1·0	0·25	0·52	40	0·46		
12	3·0	0·2	1·0	0·25	0·73	26	0·65		
13	3·5	0·2	1·0	0·26	0·70	17	0·66		
14	4·0	0·2	1·0	0·27	0·63	10	0·64	90	0·49
15	4·5	0·2	1·0	0·27	0·75	5	0·82		
16	5·0	0·2	1·0	0·27	0·72	2	0·80		
17	1·5	0·3	1·0	0·19	0·46	124	0·48	90	0·44
18	2·0	0·3	1·0	0·20	0·51	67	0·48		
19	2·5	0·3	1·0	0·21	0·58	41	0·51		
20	3·0	0·31	1·0	0·22	0·59	25	0·56		
21	3·5	0·3	1·0	0·23	0·71	16	0·67		
22	4·0	0·3	1·0	0·23	0·66	10	0·72		
23	4·5	0·3	1·0	0·24	0·70	6	0·78		
24	5·0	0·3	1·0	0·24	0·73	2	0·85		
25	1·5	0·4	1·0	0·17	0·51	121	0·49		
26	2·0	0·43	1·0	0·17	0·44	67	0·44		
27	2·5	0·4	1·0	0·18	0·56	38	0·49		
28	3·0	0·4	1·0	0·19	0·67	25	0·63	10	0·67
29	4·0	0·4	1·0	0·20	0·92	10	0·81		
30	1·5	0·5	1·0	0·14	0·49	111	0·51		
31	2·0	0·5	1·0	0·15	0·50	61	0·45		
32	2·5	0·5	1·0	0·15	0·67	38	0·58		
33	3·5	0·5	1·0	0·16	1·10	16	1·15		
34	1·5	0·6	1·0	0·11	0·55	115	0·49		
35	2·0	0·2	0·5	0·27	0·32				
36	2·0	0·5	0·3	0·35	0·25				
37	3·25	0·05	0·7	0·51	0·48				

forty separate drag determinations were made for each model at velocity intervals from about 10 cm/sec to about 250 cm/sec.

Flow visualization. Visualizing flow around an animal is important because it can indicate how drag is produced, and how change in morphology alters drag coefficient. Flow visualization has proved valuable in relating shell form to feeding habits in brachiopods (Rudwick 1961; Wallace and Ager 1966; Shiells 1968; Savage 1972), bivalves (Stanley 1970), and reef corals (Kawaguti 1943; Chamberlain and Graus 1972, 1975).

Small crystals of potassium permanganate were cemented to the venters and other critical areas of the specimens with latex glue. The crystals dissolve, releasing streams of violet dye whose downstream movements trace the pattern of flow around the specimen. Another series of tests using methylene blue and amido black dyes was done in order to observe boundary layer flow more clearly. Dye was injected from an overhead reservoir into the boundary layer at the venter of each model tested. The epoxy surface of the model was stained blue where the boundary layer is attached to the surface of the model, but remains uncoloured where the boundary layer has separated. These experiments were carried out with the low turbulence flume located in the Department of Mechanical Engineering, McMaster University.

Experimental constraints. The models were placed in lifelike positions during testing in order to simulate cephalopod swimming behaviour. All tests were done with the specimens orientated with their apertures directed posteriorly relative to water movement. The results reported here thus apply to the peculiar cephalopod habit of swimming backwards.

Wings and plates have widely differing lift and drag properties, depending on their angle of attack (Prandtl and Tietjens 1934; Hoerner 1965). The possibility of such behaviour occurring in cephalopods requires standardization of the 'swimming attitude' of the models. Thus one series of tow-tank tests was conducted in which the models were orientated with the aperture turned down and inclined about 30° to the vertical. This attitude was selected because it corresponds to the attitude of *Nautilus* when at rest (see text-fig. 3). Trueman (1941) and Raup (1967) have demonstrated that attitude depends upon the length of the body chamber so that the normal rest attitude of many species was probably different than that of *Nautilus*. Thus, a second series of tests was made in which the models were oriented as shown in
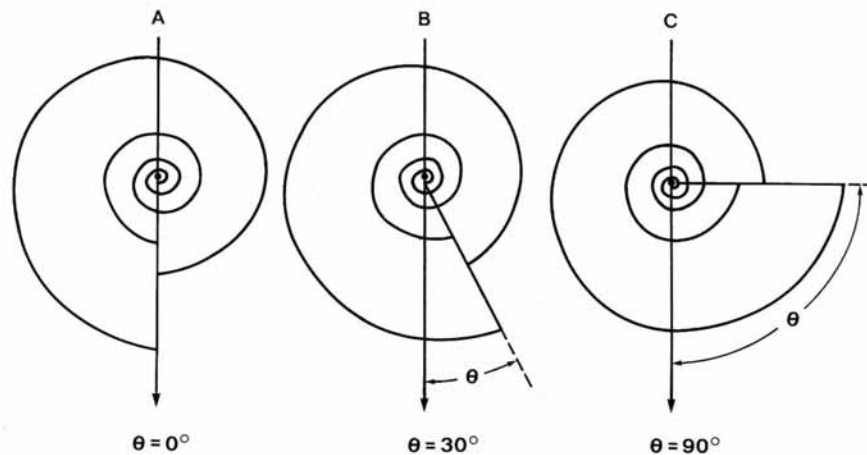

TEXT-FIG. 3. Orientation of the shell is defined as the angle (θ) between the aperture and the vertical (heavy downward arrow). A, $\theta = 0°$; B, $\theta = 30°$; C, $\theta = 90°$.

Table 1, column 7. These attitudes were calculated from the equations of Raup and Chamberlain (1967), and represent probable rest attitudes of animals having shells identical in external morphology to the models. Bidder (1962) reported that *Nautilus* 'rocks' (i.e. rotates in the vertical plane) during swimming. As both Trueman and Raup have noted, fossil ectocochliates may have behaved similarly. The effect of rocking was studied by testing three models representing widely different morphologies in orientations not covered in either of the two main series of tests (see Table 1, column 9).

SHELL FLOW PATTERNS

Drag is produced by discontinuities in the speed and direction of water moving past a body. As shown in text-fig. 1, drag depends on such major discontinuities as flow separation and wake turbulence. The manner in which shell form controls separation and turbulence is best understood by analysing shell flow patterns.

Passage of water around a cephalopod shell is shown in Plate 84 and text-fig. 4.
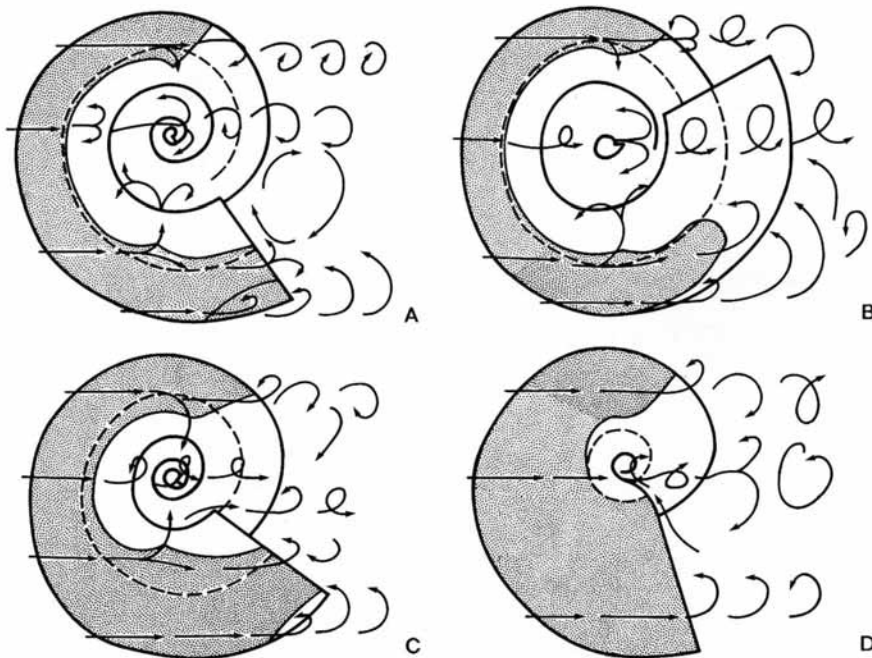
TEXT-FIG. 4. Sketch of flow lines shown in Plate 84. A, lytoceratid shell model (no. 26); B, serpenticonic shell model (no. 9); C, widely umbilicate oxyconic shell model (no. 35); D, *Nautilus pompilius* (no. 37). Area of boundary layer attachment shown by stippling. Dashed line marks umbilical shoulder on outer whorl.

I

The basic flow pattern illustrated here occurs with only minor modification for all specimens tested, and for all planispiral shells. Water passes smoothly across the venter and anterior part of the leading whorl, but in doing so loses momentum. As it approaches the umbilical shoulder, the flow stalls 'and then separates from the surface of the shell. These two events are shown in Plate 84 as a concentration of dye and distortion of the dye streams along the flank of the leading whorl. Flow is attached only to the leading part of the shell. The umbilicus and posterior portion of the shell are immersed in relatively stagnant water. Separation on the forward part of the shell creates a well-developed turbulent wake, shown in Plate 84 by swirls of dye behind the shell and in the umbilicus. Water movements near the surface of the shell are detailed in text-fig. 5. For the most part, post-separation flow at the surface consists of small, unstable vortices. Suction created behind the shell and extending into the umbilicus is sufficiently strong, however, to set up a weak, relatively stable vortex which in many shells brings water up from the wake into the umbilicus (Pl. 84, fig. 4). In addition, some water is diverted directly into the umbilicus from the flow on the outer whorl (Pl. 84, fig. 3). Thus, the major characteristics of
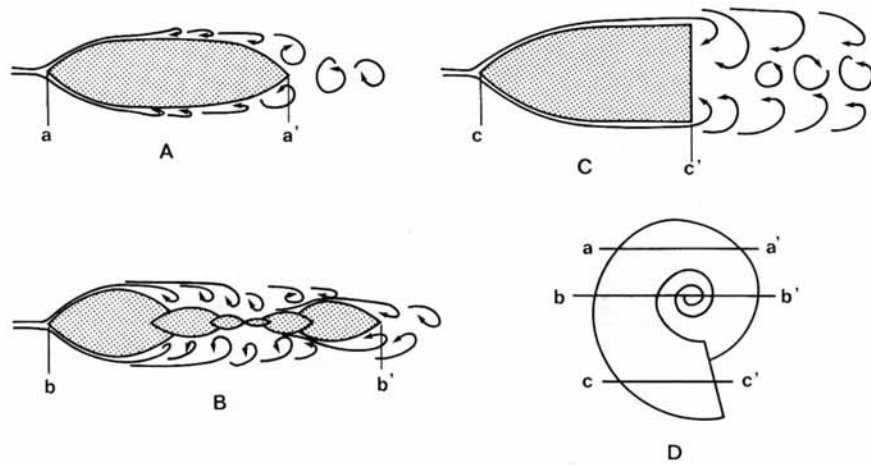
TEXT-FIG. 5. Cross-sections through flow field of model no. 35, showing details of water movement near surface of shell. A, top of shell; B, through umbilicus; C, bottom of shell and aperture; D, lateral view of shell showing position of cross-sections.
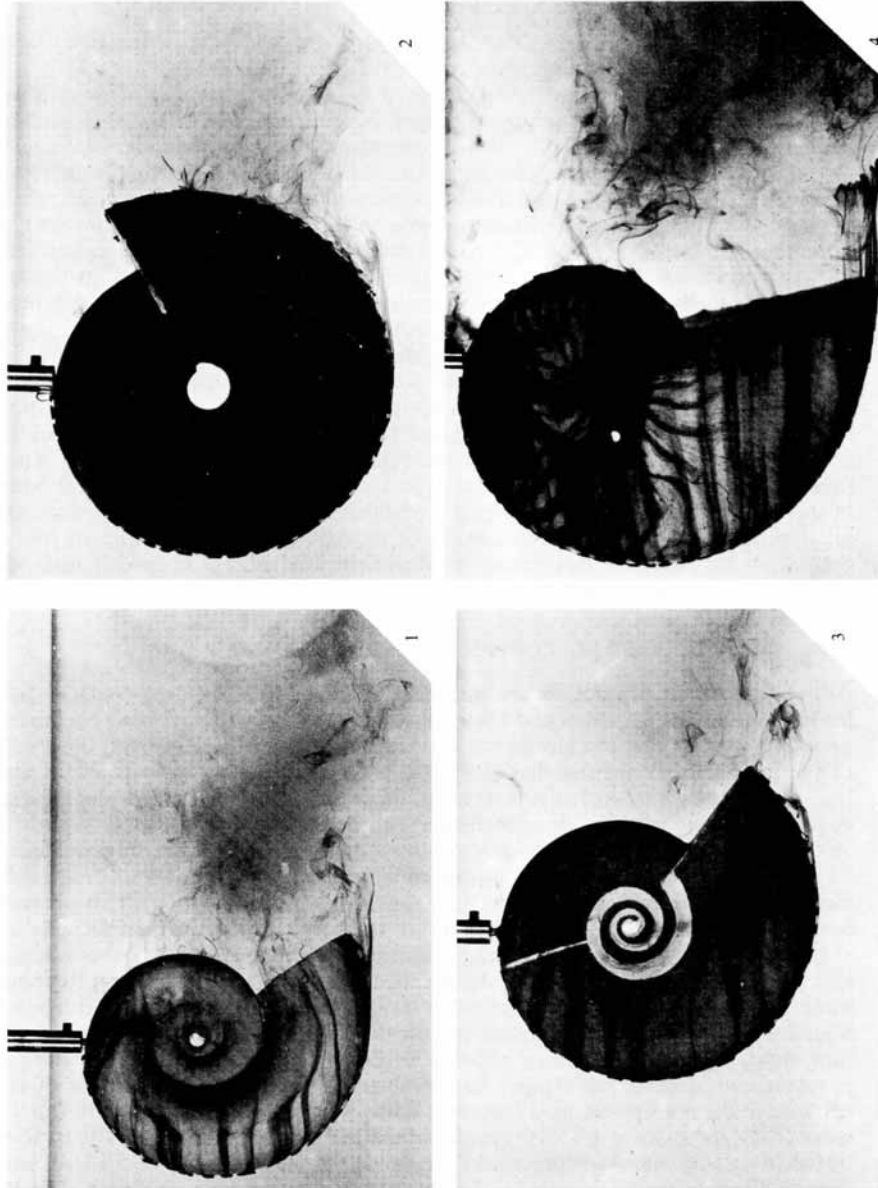
EXPLANATION OF PLATE 84

Flow fields of four specimens in rest orientation. Lines of flow made visible by violet dye bleeding from crystals of potassium permanganate cemented to venter. All ×0·25.

Fig. 1. Lytoceratid shell model (no. 26).
Fig. 2. Serpenticonic shell model (no. 9).
Fig. 3. Widely umbilicate oxycone shell model (no. 35).
Fig. 4. *Nautilus pompilius* (no. 37).

PLATE 84

CHAMBERLAIN, Flow fields of cephalopods

flow around a cephalopod shell are separation along the flank, a turbulent wake behind the flank of the leading whorl, and a turbulent umbilicus.

Shell morphology controls the structure of the flow in a number of ways. First, the position of flow separation is influenced by the curvature of the shell surface. A smooth, gently curving shell retards momentum loss in the boundary layer, and permits the flow to remain attached over more of the surface. The size of the umbilicus also influences separation. Since the flow separates at the umbilical shoulder, shells having the umbilical shoulder displaced toward the coiling axis will allow the flow to remain attached over more of the shell surface (compare Pl. 84, fig. 1, and text-fig. 4A, with Pl. 84, fig. 4, and text-fig. 4D). Shell compression is important because compressed shells invariably have more gently curving surfaces than do wider, more robust shells. Moreover, compressed shells have relatively small frontal areas (projected area in direction of flow), and therefore intercept and redirect less water per unit of shell volume. The result is smaller wakes and less flow perturbation. Finally, the absence of a solid surface behind the aperture can force premature separation over this part of the shell (Pl. 84, figs. 3 and 4; text-fig. 4C, D). The magnitude of this effect should depend on the size of the aperture relative to the size of the shell. Thus, four aspects of shell form appear to be important in structuring the flow—curvature of the shell surface, relative size of the umbilicus, degree of shell compression, and relative size of the aperture. No one factor appears to play a pre-eminent role in generating drag over the entire range of shell form studied, but in specific instances components of one or two may predominate.

DRAG COEFFICIENT AND VELOCITY

Although Schmidt did not record the effect of velocity on the drag coefficients of his four specimens, Kummel and Lloyd observed that their 'relative drag coefficient' appeared in most cases to have some dependence on velocity. However, the results of the present work suggest that shell drag coefficients are virtually constant over the velocity range studied. From text-fig. 6A, which shows a typical plot of drag coefficient versus velocity, drag coefficient can be seen to diminish only slightly as velocity increases. The other models show this same near constancy in drag coefficient. In this respect, cephalopod drag coefficients compare favourably with drag coefficients of other bodies under similar flow conditions (see text-fig. 6B). This observation should not be construed as indicating that cephalopod drag coefficients are always constant, however, since drag coefficients do change when flow conditions change. In text-fig. 6B, for example, the abrupt decrease in drag coefficient at Reynolds numbers (Re) of about 5×10^5 marks the transition between laminar and turbulent boundary layer flow. It is of interest to note that although produced by a change in flow state, this decrease can be affected by body morphology, and represents an event of considerable importance to swimmers. Drag coefficient changes of this magnitude do not appear in the present data because Reynolds numbers for this work ($5 \cdot 2 \times 10^3 \leqslant \text{Re} \leqslant 1 \cdot 8 \times 10^5$) are less than the critical value of 5×10^5, as illustrated in text-fig. 6B. At supercritical Reynolds numbers (i.e. above 5×10^5), shell drag coefficients can be expected to be lower than reported here, as sketched by the dashed line in text-fig. 6B.
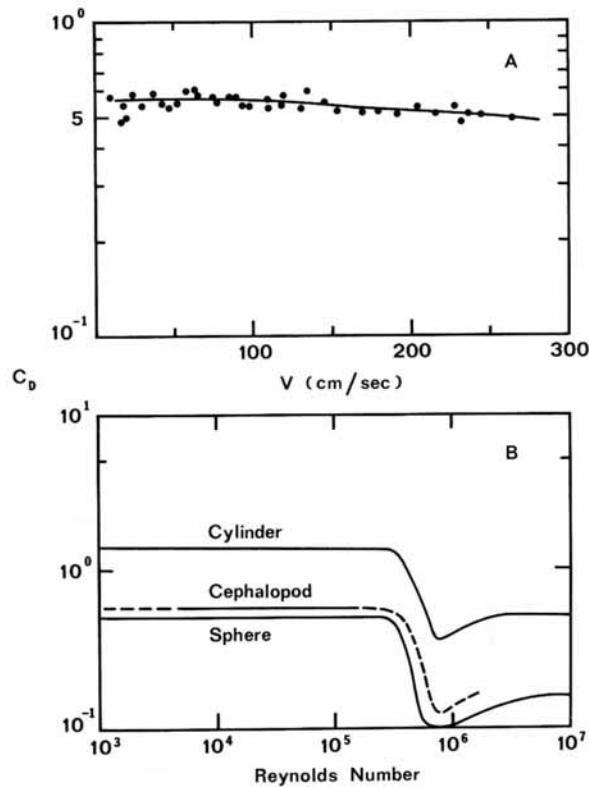
TEXT-FIG. 6. Drag coefficient of shell model 9. A, C_D versus velocity (V). Each dot represents one constant-velocity tow-tank run. B, comparison of C_D for model 9 with C_D of sphere and cylinder as a function of Reynolds number.

Since model drag coefficients are virtually constant over the entire velocity range examined here, an average drag coefficient for each model was calculated by straightforward numerical means. Average drag coefficients for all specimens are given in Table 1, and as for model 9 in text-fig. 6, apply only for laminar boundary flow (i.e. Re $< 5 \times 10^5$).

DRAG COEFFICIENT AND SHELL GEOMETRY

The basic geometrical parameters, W, D, S, and F, control flow structure by controlling shell form. Since several factors are thus involved, drag can be expected to result from a complex interaction of morphologic components. The role of any one parameter (say W) can be determined from tow-tank data from a suite of models in

which the other three parameters (S, D, and F), and orientation are constant. The role of each of the other parameters can be obtained similarly.

Whorl expansion rate (W). Text-fig. 7, shows plots of C_D against W. For each plot S, D, and orientation ($= 30°$) are constant, and variation in F is negligible. Inspection of these graphs shows that: (1) C_D varies directly with W; and (2) whorl offlap increases the rate of change of C_D with W. Thus, in shells with roughly circular whorl sections high W morphologies are generally more poorly streamlined and less efficient than low W shells.

The explanation for this relationship lies in the kind of morphological changes that result from variation in W, and in the effect of these changes on flow structure. Increase in W produces progressively greater degrees of shell inflation. Inflated shells are wider relative to their size than their deflated counterparts, and as a consequence intercept and divert a relatively larger column of water. The result is more drag and higher drag coefficients in the high W end of the morphological spectrum. Although the aperture becomes a significant morphologic feature at high W, its importance in generating drag in $S = 1$ shells is probably secondary, at least when orientation is $30°$. As shown in Plate 84, most of the flow separates before it actually reaches the aperture. The aperture operates in the wake of the umbilicus and anterior
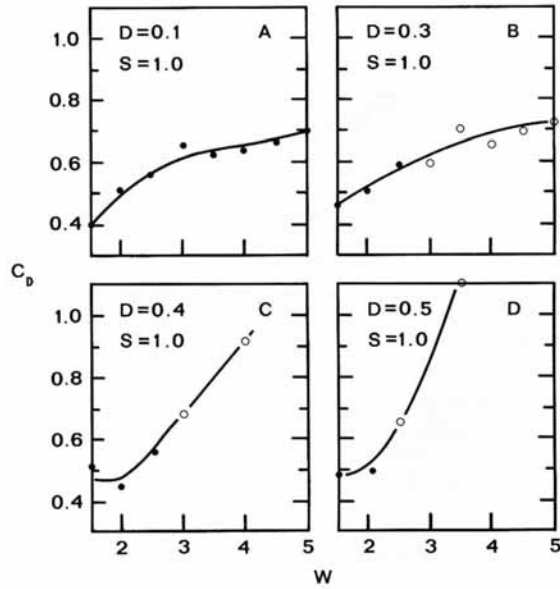
TEXT-FIG. 7. Drag coefficient (C_D) versus expansion rate (W). Dots —shells with whorl overlap. Circles—shells with whorl offlap. A, $D = 0.1$, $S = 1.0$; B, $D = 0.3$, $S = 1.0$; C, $D = 0.4$, $S = 1.0$; D, $D = 0.5$, $S = 1.0$.

part of the shell, and hence exerts relatively little influence on flow separation. As a result, the contribution of the aperture to total shell drag is probably correspondingly small.

The marked increase in drag coefficient associated with complete whorl exposure (text-fig. 7C, D) is probably brought about in two ways. The first, which could be called the 'splitter-plate' effect, derives from the influence of the shell on wake turbulence. Ordinarily, the wake consists of a fairly ordered array of vortices. When a flat plate (splitter plate) or similar object is appended to the rear of a body and aligned parallel to its direction of motion, it effectively restricts circulation in the wake and reduces vortex size (see text-fig. 8). The result is less drag. In cephalopod shells, most of the flow separates on the anterior flank, so that the umbilical and posterior regions of the shell actually operate inside the wake (Pl. 84, text-fig. 5). When the whorls overlap the trailing part of the shell acts as a splitter plate by limiting the scale of fluid movement near the shell. Whorl exposure diminishes the splitter-plate effect of the shell by permitting water to be drawn into oscillatory movements through the open spaces between successive whorls (text-fig. 9). Turbulence is enhanced and drag coefficient increases.
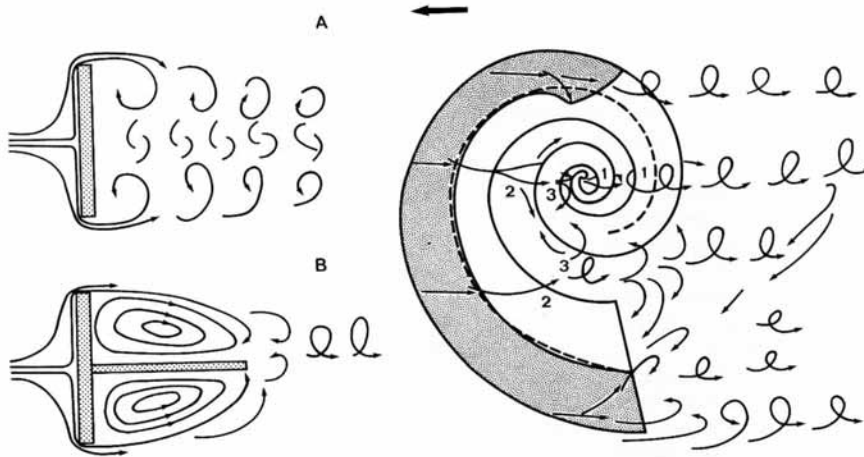
TEXT-FIG. 8. Effect of splitter plate on vortex structure in wake of perpendicular flat plate. Redrawn from fig. 3-1 of Hoerner 1965. A, perpendicular flat plate; B, perpendicular flat plate+splitter plate.

TEXT-FIG. 9. Flow pattern around a gyrocone (model no. 33). Water moves through openings between whorls. 1, flow diverts around posterior whorls. 2, flow diverts into umbilicus. 3, backflow into umbilicus.

The second way in which offlap affects the flow is by increasing the drag of the inner whorls. When whorls overlap, the inner whorls are shielded by the anterior portion of the outer whorl, and as a result should not in themselves generate much drag. Offlap reduces this 'shield effect' by exposing inner whorls to the flow. The
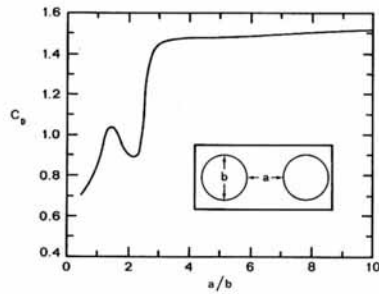
TEXT-FIG. 10. Drag coefficient of tandem cylinders as a function of distance between cylinders; C_D based on frontal area of forward cylinder. Data from Hoerner 1965. Inset shows definition of parameters: a—distance between cylinders; b—cylinder diameter.

situation is analogous to that diagrammed in text-fig. 10, for two identical cylinders arranged in tandem. As the distance between the two cylinders increases, the posterior cylinder acquires its own wake. The total drag on the two-cylinder system increases with increasing inter-cylinder distance, and reaches a maximum when the two cylinders are sufficiently distant to allow the wake elicited by the first one to subside before the passage of the second. Whorl separation never reaches the magnitudes diagrammed for cylinders, but flow visualization shows that in many gyrocones inner whorls are sufficiently distant from the leading edge of the shell, and from one another, to create their own weak wakes, and thus add to the drag of the whole shell (see text-fig. 9).

Distance to the coiling axis (D). Text-fig. 11 shows how C_D varies with D. At low $W(1\cdot5 \leqslant W \leqslant 3\cdot0)$ the magnitude of change in C_D is relatively small as long as the whorls are overlapped. For $W > 3\cdot0$, C_D increases with D, especially when offlap becomes pronounced. These observations can be interpreted in terms of variation in the size of the umbilicus. Umbilical dimensions increase from low to high D. The small umbilicus characteristic of low D, involute, shells permits the flow to remain attached to a greater portion of the shell's surface (as in Pl. 84, fig. 4; and text-fig. 5D). Separation is delayed, the umbilical drag component lessened. In contrast, high D, evolute, shells have broad umbilici and umbilical shoulders placed further forward on the shell. As in the case of the lytoceratid model illustrated in Plate 84, fig. 1, and text-fig. 5A, most of the flow is forced to separate near the leading edge of the shell. Only a small portion of the flow remains attached to posterior surfaces. The result is a gain in the umbilical drag component as D increases. Note that the position of separation on the shell depends on the size of the umbilicus, not on its morphology. The physical characteristics of the umbilicus—its depth and surface features—can be expected to exert little influence on drag.

D-related changes in shell compression and relative aperture size act in opposition to the effect of the umbilicus. Increased D results in relatively narrower shells having relatively smaller apertures (see Raup 1967). Thus, as D increases the drag components due to these two factors are reduced. Undoubtedly this inverse relationship partially offsets the effect of umbilical size, and results in the small slope in the onlap region of the $C_D - D$ plots in text-fig. 11.

Whorl shape (S *and* F). The effect on drag coefficient of variation in S can be estimated by using drag data for specimens with $S \neq 1$. Text-fig. 12A shows this data. The specimens upon which this figure is based incorporate some variation in W, D, and F, so that the curve shown in text-fig. 12A indicates only the general trend in drag coefficient as a function of S. Nevertheless, it is evident that variation in S can produce a significant decrease in shell drag coefficient. The direct relation
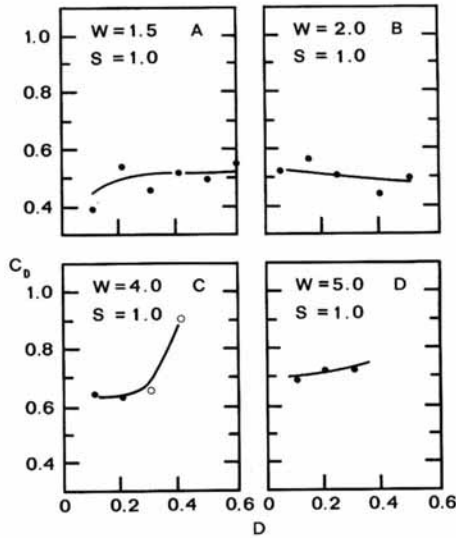
TEXT-FIG. 11
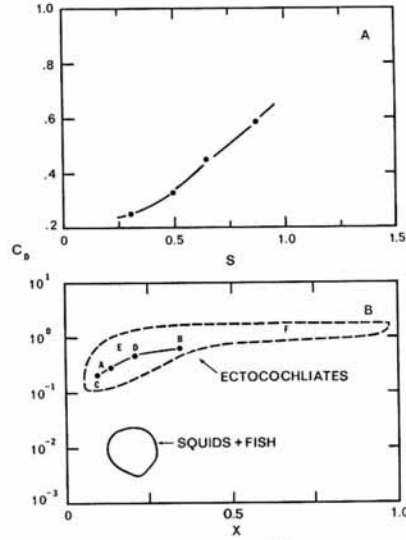
TEXT-FIG. 12

TEXT-FIG. 11. Drag coefficient (C_D) versus distance to coiling axis (D). Dots—shells with whorl overlap. Circles—shells with whorl offlap. A, $W = 1.5$, $S = 1.0$; B, $W = 2.0$, $S = 1.0$; C, $W = 4.0$, $S = 1.0$; D, $W = 5.0$, $S = 1.0$.

TEXT-FIG. 12. Drag coefficient (C_D) versus shell compression. A, data from specimens, plotted as a function of whorl shape; B, comparison of estimated ectocochliate drag coefficients with those of rapid-swimming fish and squids. X, fineness ratio. For fish and squids, X = body width/body length. For ectocochliates, X = maximum shell width/maximum shell diameter. Ectocochliate region shows approximate range in shell drag coefficient as a function of W, D, and F. Curve same as in A. Letters within ectocochliate region represent: A—evolute oxycones; B—gyrocones; C—involute oxycones; D—nautilicones; E—serpenticones; F—cadicones. Data for fish primarily from Magnan (1930) and Hertel (1966). Drag coefficients for squid estimated from performance data on *Loligo* (Trueman and Packard 1968; Packard 1969) and *Dosidicus* (Cole and Gilbert 1970).

between S and C_D can be explained in terms of shell compression. As whorls become more compressed (S decreases, F constant), the surface of the leading portion of the shell becomes more gently inclined. This diminishes the rate of momentum loss in the boundary layer, and permits the flow to remain attached for some distance into the interior of the umbilicus (Pl. 84, fig. 3; text-fig. 5C). In addition, whorl compression produces less flow disturbance as explained above. Displacement of the umbilical shoulder toward the coiling axis (S constant, F increases) may account for some of the variation in text-fig. 12A because the low S specimens in this figure (model 36 and *Nautilus*) also have high F.

The estimated effect of variation in W, D, and F at various values of S is shown in text-fig. 12B. At $S = 1$, variation in these parameters leads to a range in C_D of about 0·4–1·1, with values greater than about 0·75 being restricted to gyrocones (text-figs. 7 and 11). Shells with higher S (whorl width > whorl height) develop a

pronounced bluntness of the leading edge. High drag coefficients, which accompany bodies of such bluntness, offset any gains possibly deriving from variation in W, D, or F. The lower limit of high S (cadiconic) shells should thus be higher than when $S = 1$, as shown in text-fig. 12B. As in $S = 1$ shells, this lower limit should be found in shells with low to medium $W(1.5 \leqslant W \leqslant 3.0$, approximately) and low $D(0.1 \leqslant D)$. High F would also favour lower drag coefficient in these shells. Among high S shells, gyrocones should have the highest drag coefficients for the same reasons as discussed above, but they should not differ greatly in this respect from $S = 1$ gyrocones. Drag coefficients as large as those of gyrocones ($C_D \geqslant 1.0$) are not appreciably influenced by changes in body shape (for a two-dimensional circular cylinder ($S = 1$), $C_D = 1.1$; for a perpendicular flat plate ($S = \infty$), $C_D = 1.2$). The range in drag coefficient for high S shells thus should be about $0.6 \leqslant C_D \leqslant 1.2$.

At low S (whorl height > whorl width) drag coefficients should be correspondingly low as explained above. But within a suite of low S shells, drag coefficient will still be a function of W, D, and F, and will vary as described above for robust shells, i.e. lower drag coefficients will occur when W and D are low, and F high. In fact, the lowest shell drag coefficients, and hence most efficient of all coiled shell types, should be found among low S shells ($S \leqslant 0.25$) having very low D ($D \leqslant 0.25$) and high F ($F \approx 0.4$–0.5), i.e. involute, high-shouldered oxycones. However, it is unlikely that ectocochliate drag coefficients approach those of well-streamlined objects like wings and hydrofoils, or the bodies of rapid-swimming fish and squids, because the overall form of cephalopod shells differs from the fusiform streamlining paradigm exemplified by these other bodies by retaining two morphological irregularities— the umbilicus and aperture. Relatively little drag should be produced by separation at the umbilicus or aperture, since these features are reduced in involute oxycones. But when drag coefficient is already low, as it is in these shells (text-fig. 12A), even small drag additions significantly increase drag coefficient. The extent of umbilical and aperture separation shown in Plate 84, figs. 3 and 4, suggest that a drag coefficient of about 0.1 at $Re \approx 10^4$ is a reasonable estimate for high-shouldered, involute oxycones. Thus, the best streamlined cephalopod shells are probably more than an order of magnitude more poorly streamlined and inefficient than the bodies of modern swimmers (text-fig. 12B). For equal expenditures of propulsive energy, a fusiform fish, for example, could probably travel at least ten times faster and ten times further than an ectocochliate of equal size.

Since the low drag coefficients of involute oxycones depend to a great extent on very small umbilici, it can be expected that umbilical size will have a much greater influence on drag coefficient in compressed shells than in robust ones. As D increases from 0.05, for example, drag coefficient should rise markedly as the umbilicus widen rather than slowly as when $S = 1$. Since whorl exposure produces a large amount of turbulence regardless of whorl shape, comparatively high drag coefficients should be found among low S gyrocones. However, analogy with tandem streamlined struts (which generate less drag than a similar arrangement of cylinders, Hoerner 1965), suggests that such shells probably do not attain the high C_D values of high S gyrocones, and may not exceed $C_D \approx 0.8$.

DRAG COEFFICIENT AND BODY EXPOSURE

In modern *Nautilus* the tentacles and portions of the head can be extended outward from the aperture (Bidder 1962; Stenzel 1964; Denton and Gilpin-Brown 1966). Some evidence has been developed which suggests a similar ability in fossil ectocochliates (Flower 1955, on tentacular trace fossils; Crick 1898; Mutvei 1957, 1964; Sweet 1959; Jordan 1968, on muscle scars), and it is generally believed that most fossil forms were capable of such movement. Since any exposed surface can interact with the flow, the extension of the body behind the shell could conceivably alter drag coefficient.

In squids the head and arms continue the gentle curvature of the rest of the body, and impart a well-streamlined, fusiform body shape well adapted for efficient swimming. Presumably, the extended head and arms of fossil forms would act similarly, but to do so the exposed body must conform to two morphological requirements. First, the trailing mass of arms should approximate to a tapering fusiform shape as in squids. Secondly, the dimensions of the exposed body must be in accord with the dimensions of the shell. If the extended body is too small, it cannot fill the dead-water region behind the shell, or provide a gently curving surface to which the boundary layer can adhere. If it is too large, it will exceed the flanks of the shell, and cause more flow disturbance and drag than if it were not present at all.

Bidder (1962) and Denton and Gilpin-Brown (1966) observed that *Nautilus* holds its arms in a tapering mass, and Stürmer's recent X-ray studies (Stürmer 1970) indicates that the necessary arm arrangement may have been possible in some Devonian goniatites. Although *Nautilus* has a tendency to withdraw its arms during swimming (Bidder 1962), positioning of the arms in the proper way probably posed no great feat for most ectocochliates.

The effect of the size of the exposed body can be estimated by determining the extension required to significantly alter drag coefficient. This can be done by referring to data on aircraft and ship appendages. Text-fig. 13 presents data on fairings and circular cylinders used in experiments on drag reduction of aircraft gun barrels. It is apparent that substantial saving of energy (about 40% total barrel drag) can be obtained by placing tapered fairings behind the barrels. But it is also apparent that in order to be of service the fairings must be about as large as the barrels themselves. In particular, fairing length and width should at least equal the diameter of the barrel.

A $C_D = 1.2$

B $C_D = 0.9$

C $C_D = 0.8$

D $C_D = 0.7$

E $C_D = 0.08$
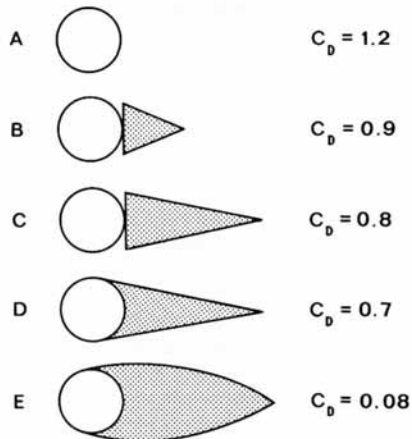
TEXT-FIG. 13. Effect of tapered fairings on subcritical drag coefficients of aircraft gun barrels. Redrawn from figs. 13-50 and 13-51 of Hoerner 1965. A, barrel cross-section; B, C, D, barrel+tapered fairings of various sizes (in cross-section); E, barrel+streamlined sleeve.

Shells are not gun barrels, nor are body parts fairings, but the analogy is a useful one because it tells us that exposed parts of the body must be approximately the same size as the shell itself to obtain a significant reduction in drag coefficient. Lesser degrees of extension will result in only small or insignificant gains in energy economy because the afterbody is not large enough to give a fully developed fusiform shape to the shell-animal combination. In addition, the extended parts must cover the entire rear of the shell, not just the aperture, and should extend into the umbilicus to ensure a smooth, continuous afterbody profile. Otherwise, gaps and surface discontinuities left between the shell and body create obstacles that cause flow separation, and thereby minimize any beneficial effect body extension may have. The body of *Nautilus* is far too small to meet these criteria, even when fully extended. It would appear that *Nautilus* cannot derive much advantage from this effect.

Although our knowledge of the anatomy of fossil ectocochliates is fragmentary at best, there is ample evidence which shows that the afterbody in fossil forms also was not large enough to fully exploit this mode of drag reduction. For example, the presence of colour markings (Ruedemann 1921; Schindewolf 1928; Foerste 1930; Spath 1935) and pre-mortal epizoans (Dunbar 1928; Lange 1932; Schindewolf 1934; Seilacher 1960; Merkt 1966; and Meischner 1968) shows that shell surfaces which should have been covered by such a ponderous afterbody were actually free of even a temporary covering of flesh. Moreover, the excellent reconstructions of ectocochliate anatomy given by Mutvei (1957, 1964), Jordan (1968), and Lehmann (1971, 1972), and such rare anatomical insights as those of Flower (1955), Müller (1969), and Wetzel (1969) indicate that the fossil animal was probably fairly similar to modern *Nautilus* both in general anatomy and in the relation of the animal to its shell. We can conclude that, in general, body extension probably plays little part in altering drag coefficient in either fossil or modern ectocochliates. The statements of Schmidt (1930) that the soft parts are hydrodynamically more meaningful than many variations of the shell, or of Geczy (1960) that because of body extension shell drag does not express the drag of the whole animal, are clearly excessive.

High-shouldered, involute oxycones may be an exception to this general rule, but only if body extension were sufficient to provide a fully developed afterbody behind the aperture. In other shells, the effectiveness of such an afterbody behind the aperture would be small because the resultant drag loss would be overwhelmed by turbulence generated by other sources (e.g. umbilicus, blunt leading edge, spines, etc.). In high-shouldered, involute oxycones turbulence due to these other sources is minimal so that a considerable percentage of the total turbulence may be eliminated by body extension, and the resulting gain in energy economy may be substantial. In contrast, the poorly streamlined gyroconic form of Stürmer's goniatites suggest that these animals could not profit hydrodynamically from extension of their bodies, although the degree of extension indicated in Stürmer's radiograph is certainly sufficient to form a complete afterbody behind the aperture.

DRAG COEFFICIENT AND SHELL ORIENTATION

As in any body which is not perfectly symmetrical in three dimensions, drag elicited by a cephalopod shell will vary as a function of its orientation relative to the flow.

The shape of the shell (and therefore streamlining) does not change, but the position of individual morphologic elements with respect to the flow may vary substantially. Fossil cephalopods were probably able to alter their orientation in the manner of *Nautilus*, so that it is of some value to examine the effect of orientation in more detail.

TABLE 2. Difference in model drag coefficients between attitudes of 30° and calculated rest attitude. Positive values indicate C_D in rest position exceeds C_D in 30° position. Negative values indicate C_D in 30° position exceeds C_D in rest position.

W	D					
	0·1	0·2	0·3	0·4	0·5	0·6
1·5	−0·02	−0·03	+0·02	−0·02	+0·02	−0·06
2·0	−0·06	−0·06	−0·03	0·0	−0·05	
2·5	−0·09	−0·06	−0·07	−0·07	−0·09	
3·0	−0·08	−0·08	−0·03	−0·04		
3·5	+0·12	−0·04	−0·04		−0·05	
4·0	+0·13	+0·01	+0·08	+0·05		
4·5	+0·18	+0·07	+0·08			
5·0	+0·26	+0·08	+0·12			

Table 2 shows the extent of the difference between drag coefficients for orientations of 30° and calculated rest attitude (which vary between 1° and 124° depending on W and D, see Table 1). In most cases the amount of variation in drag coefficient is relatively small. Low W shells generally have somewhat lower drag coefficients in their rest attitudes, while high W shells have higher drag coefficients. No obvious trend occurs as a function of D. As shown in text-fig. 14, these differences do not significantly alter the nature of the dependence of drag coefficient on shell geometry. Compared to shell form, orientation appears to be a comparatively minor hydrodynamic factor.

Text-fig. 15 shows how drag coefficient varies as a function of attitude in low and high W shells. In both cases, drag coefficient is minimum when the aperture is aligned parallel with the flow (i.e. at 90°). Minimal drag coefficients in this configuration are probably due to: (1) virtual elimination of the aperture as a hydrodynamic factor; and (2) shell asymmetry. When the aperture is inclined at an angle of less than 90° (as in text-fig. 3A, B), truncation of the shell surface at the aperture margin forces the flow in this region to separate prematurely (Pl. 84, figs. 1, 3, and 4; and text-fig. 5A, C, D). When attitude is greater than 90°, the aperture impinges directly on the flow, and forces the flow to diverge around it (Pl. 84, fig. 2; and text-fig. 5B). In both cases, an inclined aperture results in more turbulence, and hence more total shell drag, than when the aperture is parallel. The effect of shell symmetry can be illustrated by considering a scallop shell. When a scallop is held in its normal swimming position, that is, with the commissure parallel to flow (attitude = 90°), it will disturb far less water than when the commissure is inclined to the flow (for example, commissure perpendicular; orientation = 0°). Similar discrepancies as a function of attitude should occur for coiled cephalopods because a cephalopod shell, like a scallop shell, is symmetrical in only one plane (plane of bilateral
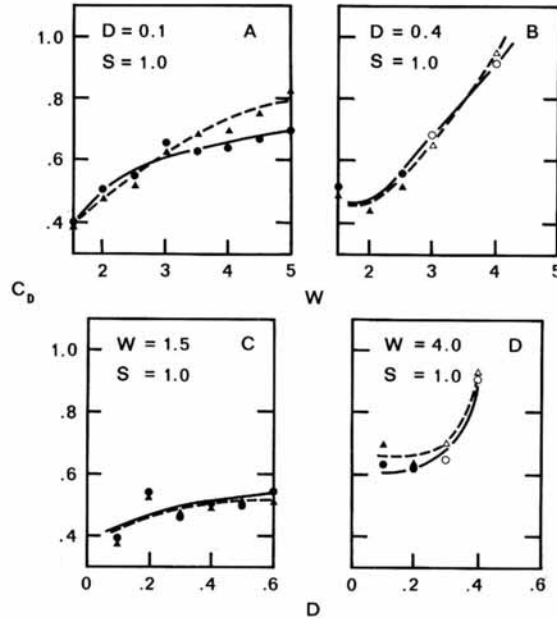
TEXT-FIG. 14. Comparison of drag coefficient (C_D) for shell models
in calculated rest orientation and 30° orientation. Dots—30°, whorl
onlap. Circles—30°, whorl offlap. Solid triangles—rest attitude,
whorl onlap. Open triangles—rest attitude, whorl offlap. A, C_D
versus W, $D = 0·1$, $S = 1·0$; B, C_D versus W, $D = 0·4$, $S = 1·0$;
C, C_D versus D, $W = 1·5$, $S = 1·0$; D, C_D versus D, $W = 4·0$, $S = 1·0$.

symmetry). Rotation around the coiling axis will alter the configuration a cephalo-
pod presents to the flow in the same way as for a scallop shell. However, the effect
on drag coefficient should be much smaller in cephalopods because their low expan-
sion rates render cephalopod shells more nearly symmetrical with respect to the axis
of rotation.

The way in which drag coefficient varies in Table 2 can be explained as the result
of how rest orientations differ with respect to the 30° orientation of *Nautilus*. The
calculated rest attitudes of low W specimens are near 90° (Table 1). Drag coefficients
near 90° are generally lower than at 30° as explained above, so that the drag coefficient
differentials of low W shells are negative as illustrated in Table 2. The rest attitudes
of high W shells are less than 30° (Table 1), and hence their drag coefficient dif-
ferentials are positive (Table 2).

Text-fig. 15 also shows that attitudinal variation in drag coefficient is greater for
high W shells. This probably results from the high degree of inflation characteristic
of high W morphology. High W shells have large apertures and rapidly enlarging
whorls, both of which make the configurations such shells present to the flow as a
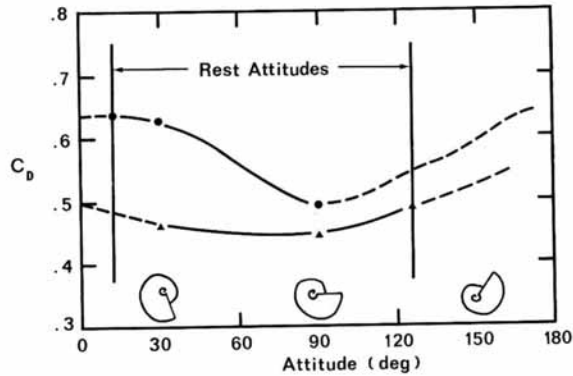
TEXT-fiG. 15. Drag coefficient (C_D) versus attitude for high W (dots) and low W (triangles) shells.
High W shell-model no. 14, low W shell-model no. 17.

function of orientation, and attendant flow disruption, highly variable (for cephalopods). In contrast, low W shells have relatively small apertures and whorls which expand very gradually (when $W = 1$, a logarithmic spiral decays into a circle, and shell form would become toroidal, i.e. symmetrical with respect to the coiling axis). Since low W shells are thus morphologically more uniform, attitudinal variation will have a smaller effect on drag coefficient.
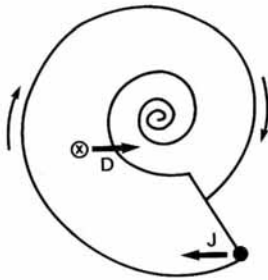
TEXT-FIG. 16. Effect of drag and thrust on attitude. Shell moving from right to left. Drag (D) acts backward from centre of dynamic pressure ($\otimes$), which lies near centre of gravity near coiling axis. Thrust (J) acts in direction of motion from point of application ($\bullet$) at ventral margin of aperture. Lines of action of the forces set up a moment which causes a clockwise rotation of the shell (arrows).

The rocking associated with swimming in *Nautilus* is associated with variations in instantaneous thrust resulting from pulsations of the hyponome. Since total drag acts near the centre of the shell and thrust is applied at the ventral margin of the aperture (see text-fig. 16), the two forces set up a moment which rotates the shell away from its rest position. As thrust and drag increase, the angular rotation should increase correspondingly. Analysis of a movie film of *Nautilus* swimming supports this interpretation. The relation between lines of action and points of application of drag and thrust should be the same as that shown in text-fig. 16 as long as rest orientation lies between 0° and 90°. Since calculations on static stability (Trueman 1941; Raup 1967; J. S. Weaver, pers. comm.), and experiments on floating orientation (Reyment 1958, 1973; Raup 1973; Weaver and Chamberlain 1976) show that most coiled cephalopods probably had rest orientations within these limits (the only exceptions may have been shells with $1 \cdot 25 \leqslant W \leqslant 1 \cdot 75$, Raup 1967), it appears that most shells must rotate like *Nautilus* during swimming. Thus it follows that the lowest effective drag coefficient of a cephalopod shell (with the above exception) will be that measured in its rest position

because rotation during swimming always alters attitude (text-fig. 16) in the direction of greater drag coefficient (text-fig. 15). Therefore the faster an ammonoid or nautiloid swam, the more closely its attitude must have approached 0°, and the greater its effective drag coefficient would have become. This in itself may have placed upper limits on the performance of fossil cephalopods, especially those with low drag coefficients (e.g. involute oxycones).

CONCLUSIONS

Tow-tank measurement of shell drag coefficient (C_D), and flow visualization of shell flow patterns suggest the following:

1. Flow around coiled cephalopod shells is characterized by three kinematic properties:
   - (a) boundary layer separation along the flank of the outer whorl approximately coincident with the outer umbilical shoulder;
   - (b) a turbulent wake behind the shell caused by separation;
   - (c) turbulent, unsteady vortices in the umbilicus.

2. Low drag coefficients are produced by shell morphologies which delay separation, and generate little turbulence. Shell drag coefficient is nearly independent of velocity for Reynolds numbers less than about 3×10^5, and in this respect is comparable to drag coefficients of other blunt, rounded bodies in subcritical flow.

3. The following trends in drag coefficient occur as a function of expansion rate (W) and umbilical size (D) in shells with roughly circular whorl sections:
   - (a) C_D increases from about 0·45 in low W (deflated) shells to 0·9 in high W (inflated) shells;
   - (b) C_D generally increases with D (i.e. as umbilicus enlarges);
   - (c) whorl offlap results in comparatively high $C_D (\approx 1·1)$.

4. Variation in whorl compression (S) causes order of magnitude changes in drag coefficient. Involute oxycones ($D < 0·1$; $S \approx 0·2$) probably have the lowest $C_D (\approx 0·1)$ of all cephalopod shells. Depressed cadicones ($S > 1$) have high $C_D (\approx 1·0)$. While gross change in shell form may not greatly affect C_D when S is high ($S \approx 1$), the C_D's of low S (compressed) shells are very sensitive to changes in morphology.

5. Drag coefficients of cephalopod shells are more than an order of magnitude higher than the drag coefficients of the bodies of rapid-swimming fish, mammals, and squids. This means that even the best streamlined shelled cephalopod (involute oxycone) is at least ten times more inefficient than these animals. Depressed cadicones are probably more than 100 times less efficient.

6. Decrease in drag coefficient as a function of increasing whorl compression is due to increasing gentleness of the surface curvature of the shell, and to removal of the position of maximum shell width backward from the leading edge of the shell. Increase in drag coefficient with W is due to increase in frontal area and relative size of the aperture. Increase in drag coefficient with D is due to increase in the size of the umbilicus.

7. Drag coefficient varies with shell orientation because shells are not morphologically uniform in three dimensions. The lowest drag coefficients occur when the aperture is orientated parallel to the flow and increases as the aperture rotates away from this position. The magnitude of this increase is greatest in high W shells. However, the over-all change in drag coefficient is relatively minor compared to variation due to shell form. For most shells the rotational moment due to drag and thrust is such that the lowest effective drag coefficient occurs when shells are orientated in their rest position. This implies that drag coefficient increases with swimming speed.

8. Analogy with ship and aircraft appendages suggests that extension of the body behind the shell has virtually no effect on drag coefficient for most ectocochliates.

Like any high performance machine, rapid swimmers must be efficient. They do not waste their limited supply of propulsive energy in unproductive ways. Their bodies are well streamlined because such shapes have the highest hydrodynamic efficiencies. Inasmuch as body shape and swimming ability are so closely related, understanding the hydrodynamic properties of shell form is an important step toward deducing the swimming ability and life habits of fossil cephalopods.

REFERENCES

ALEXANDER, R. MCN. 1967. *Functional Design in Fishes.* Hutchinson, London, 160 pp.
—— 1968. *Animal Mechanics.* University of Washington Press, Seattle, 422 pp.
BAYER, U. 1970. Anomalien bei Ammoniten des Aaleniums und Bajociums und ihre Beziehung zur Lebensweise. *Neues Jahrb. Geol. Palaont., Abh.* **135**, 19–41.
BIDDER, A. M. 1962. Use of the tentacles, swimming, and buoyancy control in the pearly Nautilus. *Nature, London,* **196**, 451–454.
CHAMBERLAIN, J. A., Jun. 1969. Technique for scale modelling of cephalopod shells. *Palaeontology,* **12**, 48–55.
—— and GRAUS, R. R. 1972. Flume study of water flow patterns in branched reef corals. *Geol. Soc. Amer., Program Ann. meeting for 1972,* 468. (Abstract.)
—— —— 1975. Water flow and hydromechanical adaptations of branched reef corals. *Bull. Mar. Sci.* **25**, 112–125.
COLE, K. S. and GILBERT, D. L. 1970. Jet propulsion in squid. *Biol. Bull.* **138**, 245–246.
CRICK, G. C. 1898. On the muscular attachment of the animal to its shell in some fossil cephalopoda (Ammonoidea). *Trans. Linn. Soc. London,* **7**, 71–113.
DENTON, E. J. and GILPIN-BROWN, J. B. 1966. On the buoyancy of the pearly Nautilus. *Jour. Mar. Biol. Ass. U.K.* **46**, 723–759.
DUNBAR, C. O. 1928. On an ammonite shell investing commensal Bryozoa. *Amer. J. Sci.* **16**, 164–165.
FLOWER, R. H. 1955. Trails and tentacular impressions of orthoconic cephalopods. *J. Paleont.* **29**, 857–867.
FOERSTE, A. G. 1930. The color patterns of fossil cephalopods and brachiopods, with notes on gastropods and pelecypods. *Univ. Michigan Mus., Paleont. Contr.* **3**, 109–150.

K

GECZY, B. 1960. On the way of life of the Neoammonoids. *Foldt. Kozl.* **90**, 200-203.

HERTEL, H. 1966. *Structure, Form, and Movement.* Reinhold, New York, 251 pp.

HOERNER, S. F. 1965. *Fluid Dynamic Drag*, publ. by author, Midland Park, N.J., 432 pp.

JORDAN, R. 1968. Zur Anatomie mesozoischer Ammoniten nach den Strukturelementen der Gehäuse-Innenwand. *Beih. Geol. Jahrb.* **77**, 1-64.

KAWAGUTI, S. 1943. Growth form of reef corals in relation to water currents. *Nat. Hist. Soc., Taiwan Jour.* **33**, 263-267.

KUMMEL, B. and LLOYD, R. M. 1955. Experiments on relative streamlining of coiled cephalopod shells. *J. Paleont.* **29**, 159-170.

LANGE, W. 1932. Über Symbiose von *Serpula* mit Ammoniten im unteren Lias Norddeutschlands. *Z. d. geol. Ges.* **89**, 229-234.

LEHMANN, U. 1971. New Aspects in Ammonite biology. *Proc. North Amer. Paleont. Conv.* Part I, 1251-1269.
—— 1972. Aptychen als Kieferelemente der Ammoniten. *Z. Paläont.* **46**, 34-48.

MAGNAN, A. 1930. Les caracteristiques geometriques et physiques des poissons. *Ann. Sci. Nat., Zool.* Ser. 10, **13**, 355-489.

MEISCHNER, D. 1968. Perniciöse Epökie von *Placunopsis* auf *Ceratites. Lethaia,* **1**, 156-174.

MERKT, J. 1966. Über Austern und Serpeln als Epöken auf Ammonitengehäusen. *Neues. Jb. Geol. Paläont. Abh.* **125**, 467-479.

MÜLLER, A. 1969. Ammoniten mit 'Eierbeutel' und die Frage nach dem Sexualdimorphismus der Ceratiten (Cephalopoda). *D. Akad. Wiss. Berlin, Msh.* **11**, 411-420.

MUTVEI, H. 1957. On the relations of the principal muscles to the shell in *Nautilus* and some fossil nautiloids. *Ark. Min. Geol.* **2**, 219-254.
—— 1964. Remarks on the anatomy of recent and fossil cephalopoda. *Stockh. Contr. Geol.* **11**, 79-102.
—— and REYMENT, R. A. 1973. Buoyancy control and siphuncle function in ammonoids. *Palaeontology,* **16**, 623-636.

PACKARD, A. 1969. Jet propulsion and the giant fibre response of *Loligo. Nature, London,* **221**, 875-877.

PETRICONI, V. 1971. Zur Schwimmrichtung der Belemniten und Ökologie hohrender Cirripeden. *Palaeogeog. Palaeoclim. Palaeoecol.* **9**, 133-148.

PRANDTL, L. and TIETJENS, O. J. 1934. *Applied Hydro- and Aero-mechanics.* Dover, New York, 311 pp.

RAUP, D. M. 1961. The geometry of coiling in gastropods. *Proc. natn. Acad. Sci. U.S.A.* **47**, 602-607.
—— 1962. Computer as aid in describing form in gastropod shells. *Science,* **138**, 150-152.
—— 1966. Geometric analysis of shell coiling: general problems. *J. Paleont.* **40**, 1178-1190.
—— 1967. Geometric analysis of shell coiling: coiling in ammonoids. Ibid. **41**, 43-65.
—— 1973. Depth inferences from vertically imbedded cephalopods. *Lethaia,* **6**, 217-226.
—— and CHAMBERLAIN, J. A., Jun. 1967. Equations for volume and center of gravity in ammonoid shells. *J. Paleont.* **41**, 566-574.
—— and MICHELSON, A. 1965. Theoretical morphology of the coiled shell. *Science,* **147**, 1294-1295.

REYMENT, R. A. 1958. Some factors in the distribution of fossil cephalopods. *Stockh. Contr. Geol.* **1**, 97-184.
—— 1973. Factors in the distribution of fossil cephalopods. 3. Experiments with exact shell models of certain shell types. *Bull. geol. Inst. Univ. Uppsala,* N.S. **4**, Part 2, 7-41.

ROLL, A. 1935. Über Frasspuren in ammonitenschalen. *Zentralbl. Min. Geol.* Abt. B, **36**, 120-124.

RUDWICK, M. J. S. 1961. The feeding mechanism of the Permian brachiopod *Prorichthofenia. Palaeontology,* **3**, 450-471.

RUEDEMANN, R. 1921. On color bands in Orthoceras. *Bull. N.Y. State Mus., 16th Ann. Rpt.* No. 227-228, 79-88.

SAVAGE, N. M. 1972. Some observations on the behavior of the Recent brachiopod *Megerlina pisum* under laboratory conditions. *Lethaia,* **5**, 61-67.

SCHINDEWOLF, O. H. 1928. Über Farbstreifen bei *Amaltheus* (*Paltopleuroceras*) *spinatum* (Brug.). *Z. Paläont.* **10**, 136-143.
—— 1934. Über Epöken auf Cephalopoden-Gehäusen. Ibid. **16**, 15-31.

SCHMIDT, H. 1930. Über die Bewegungsweise der Schalencephalopoden. Ibid. **12**, 194-208.

SCOTT, G. 1940. Paleoecological factors controlling the distribution and mode of life of Cretaceous ammonoids in the Texas area. *J. Paleont.* **14**, 299-323.

SEILACHER, A. 1960. Epizoans as a key to ammonoid ecology. Ibid. **34**, 189-193.

SEILACHER, A. 1968. Swimming habits of belemnites recorded by boring barnacles. *Palaeogeog. Palaeoclim. Palaeoecol.* **4**, 279–285.

SHIELLS, K. A. G. 1968. *Kochiproductus coronus* sp. nov. from the Scottish Visean and a possible mechanical advantage of its flange structure. *Trans. R. Soc. Edinb.* **67**, 477–507.

SPATH, L. F. 1935. On color markings in ammonites. *Ann. Mag. Nat. Hist.* Ser. 10, **15**, 395–398.

STANLEY, S. M. 1970. Relation of shell form to life habits in the bivalve mollusca. *Mem. Geol. Soc. Amer.* **125**, 296 pp.

STENZEL, H. B. 1964. Living *Nautilus*. *In* MOORE, R. C. (ed.), *Treatise on Invertebrate Paleontology*, Part K, Mollusca 3, University of Kansas Press, Lawrence, Kansas, 59–93.

STÜRMER, W. 1970. Soft parts of cephalopods and trilobites: some surprising results of X-ray examinations of Devonian slates. *Science*, **170**, 1300–1302.

SWEET, W. C. 1959. Muscle-attachment impressions in some Paleozoic nautiloid cephalopods. *J. Paleont.* **33**, 293–304.

TRUEMAN, A. E. 1941. The ammonite body-chamber, with special reference to the buoyancy and mode of life of the living ammonoid. *Q. Jl Geol. Soc. Lond.* **96**, 339–383.

TRUEMAN, E. R. and PACKARD, A. 1968. Motor performances of some cephalopods. *Jour. Exp. Biol.* **49**, 495–508.

WALLACE, P. and AGER, D. V. 1966. Flume experiments to test the hydrodynamic properties of certain spiriferid brachiopods with reference to their supposed life orientation and mode of feeding. *Proc. Geol. Soc. Lond.* **1635**, 160–163.

WEAVER, J. S. and CHAMBERLAIN, J. A., Jun. 1976. Equations of motion for post-mortem sinking of cephalopod shells and the sinking of *Nautilus*. *Paleobiology*, **2**, 8–18.

WESTERMANN, G. E. G. 1954. Monographie der Otoitidae (Ammonoidea). *Beih. Geol. Jahrb.* **15**, 364 pp.

—— 1973. Strength of concave septa and depth limits of fossil cephalopods. *Lethaia*, **6**, 383–403.

WETZEL, W. 1969. Seltene Wohnkammerinhalte von Neoammoniten. *Neues Jb. Geol. Paläont.*, *Mh.* 46–53.

J. A. CHAMBERLAIN, JUN.

Department of Geology
Brooklyn College of the City University of New York
Brooklyn, New York 11210
U.S.A.